DRAFT VERSION NOVEMBER 25, 2014
Preprint typeset using LaTeX style emulateapj v. 5/2/11

arXiv:1405.6029v2 [astro-ph.GA] 24 Nov 2014

SECULAR EVOLUTION OF BINARIES NEAR MASSIVE BLACK HOLES: FORMATION OF COMPACT BINARIES, MERGER/COLLISION PRODUCTS AND G2-LIKE OBJECTS

SNEZANA PRODAN[1], FABIO ANTONINI[1,2] & HAGAI B. PERETS[3]

Draft version November 25, 2014

ABSTRACT

Here we discuss the evolution of binaries around MBH in nuclear stellar clusters. We focus on their secular evolution due to the perturbation by the MBH, while simplistically accounting for their collisional evolution. Binaries with highly inclined orbits in respect to their orbit around the MBH are strongly affected by secular processes, which periodically change their eccentricities and inclinations (e.g. Kozai–Lidov cycles). During periapsis approach, dissipative processes such as tidal friction may become highly efficient, and may lead to shrinkage of a binary orbit and even to its merger. Binaries in this environment can therefore significantly change their orbital evolution due to the MBH third-body perturbative effects. Such orbital evolution may impinge on their later stellar evolution. Here we follow the secular dynamics of such binaries and its coupling to tidal evolution, as well as the stellar evolution of such binaries on longer time-scales. We find that stellar binaries in the central parts of NSCs are highly likely to evolve into eccentric and/or short period binaries, and become strongly interacting binaries either on the main sequence (at which point they may even merge), or through their later binary stellar evolution. The central parts of NSCs therefore catalyze the formation and evolution of strongly interacting binaries, and lead to the enhanced formation of blue stragglers, X-ray binaries, gravitational wave sources and possible supernova progenitors. Induced mergers/collisions may also lead to the formation of G2-like cloud-like objects such as the one recently observed in the Galactic center.

Subject headings: binaries: close — stellar dynamics— celestial mechanics— stars: binaries: general— Galactic Center

1. INTRODUCTION

The majority of stars are believed to be in binaries or higher multiplicity systems, both in the field and in the dense stellar environments of globular clusters and galactic nuclei. In the inner parts of the nuclear stellar cluster (NSC) of the Galactic center (GC; within ~ 1 pc) the gravitational potential is dominated by the central massive black hole (MBH). Binaries in the NSC are bound to the MBH and effectively form hierarchical triple systems with the MBH (i.e. the binary orbit around the MBH is the outer orbit of the triple). If the orbit of a binary is highly inclined with respect to its orbit around the MBH, strong oscillations of the inner orbit eccentricity and mutual inclination are induced on secular timescale. The secular timescale is often shorter then the timescale over which gravitational interactions with background stars would significantly affect either the internal or the external orbit of the binary. These oscillations are known as Kozai–Lidov (KL) cycles (Lidov 1962; Kozai 1962). The induced high eccentricities could lead to strong interactions between the stellar binary components, producing significant orbital shrinkage, as well as potentially affecting the later binary stellar evolution.

Antonini & Perets (2012, AP12) explored the evolution of compact binaries (white dwarfs, neutron stars and black holes) orbiting the MBH. AP21 followed the coupled KL evolution and the gravitational wave (GW) emission was followed, while considering the potentially limited lifetime of binaries due their softening and final destruction through encounters with stars in the nuclear cluster. It was shown that such coupled evolution could significantly affect the binary evolution and enhance the rate of GW sources formation, as well as change their characteristics, in particular producing eccentric GW sources. Furthermore, AP12 discovered the regime of quasi-KL evolution occurring for weakly hierarchical triples. During such evolution, the eccentricity of the inner binary experiences significant changes on dynamical timescale due to the perturbations from a third body. Such changes in the eccentricity are no longer of purely secular nature and therefore one should be cautious when numerically treating such systems. Some of the implications of this discovery are discussed in Antonini et al. (2014) as well.

Here we expand on AP12 and Antonini et al. (2010) and explore the evolution of main-sequence (MS) binaries near MBHs and environments similar to the NSC of the Milky-way. As we discuss in the following, the coupling of KL-cycles and tidal friction (Kozai-Lidov cycles+tidal friction; KCTF) in such binaries has an important impact on the evolution of the binary components, leading to orbital shrinking and even mergers (a scaled up version of the KCTF in stellar triples; e.g. Eggleton 2006; Fabrycky & Tremaine 2007; Perets & Fabrycky 2009; Perets & Naoz 2009; Prodan & Murray 2012; Prodan et al. 2013; Prodan & Murray 2014; Katz & Dong 2012; Naoz et al. 2013a,b; Naoz & Fabrycky 2014). We follow the KCTF evolution of the binaries until they merge or until at least one of the binary components evolves beyond

[1] Canadian Institute for Theoretical Astrophysics, 60 St. George Street, University of Toronto, Toronto, ON M5S 3H8, Canada; sprodan@cita.utoronto.ca, antonini@cita.utoronto.ca
[2] Departimento di Fisica, Universita' di Roma 'La Sapienza', P.le A. Moro 5, I-00185, Rome, Italy
[3] Deloro Fellow; Physics Department, Technion - Israel Institute of Technology, Haifa, Israel 32000

the MS, at which point we stop the full dynamical evolution of these binaries.Their later stellar evolution is then followed in isolation (the full coupling of secular dynamical triple evolution with binary stellar evolution is beyond the scope of this paper, and we only follow this limited, simplified approach). Though highly simplified, this method allows us to track for the first time the effects of the KCTF evolution during the MS phase, and their implications for the long term stellar evolution of NSC binaries.

In Section 2 we describe the KL dynamics in the presence of additional forces and dissipation due to tides, and describe the relevant timescales. The choices of the initial conditions and the binary stellar evolution parameters are discussed in Section 3. In Section 4 we describe the results of numerical integration of the equations of motion using both orbit-averaged and N-body approach, as well as results of the binary stellar evolution. We discuss our findings in Section 5 and summarize.

2. THREE BODY DYNAMICS IN THE PRESENCE OF ADDITIONAL FOCES

2.1. *The Kozai–Lidov mechanism*

We consider triple systems in hierarchical configurations, i.e. system in which the ratio between the outer binary semi-major axis (SMA) and the inner binary SMA is large. In such systems even small gravitational perturbations by the outer third body can significantly affect the inner binary orbital evolution on long enough secular timescales. The changes in the orbital elements of the inner binary can be particularly dramatic when the mutual inclination between the two orbits is high. Such configuration leads to the exchange of angular momentum between the inner and the outer orbits, resulting in periodic oscillations in the eccentricity of the inner orbit as well as the mutual inclination. The critical mutual inclination for having these oscillations, known as KL cycles (Kozai 1962), is $i_{crit} \approx 39.2^o$ (for initially circular orbits of the inner binary). If the orbits are prograde ($i_{crit} \leq i \leq 90^o$) these cycles are out of phase: when the eccentricity reaches its maximum, the mutual inclination reaches its minimum and vice versa. If the orbits are retrograde ($i > 90^o$) these cycles are in phase: both the eccentricity and the mutual inclination reach maximum values simultaneously. The period of a KL cycle are much longer then the period of both the inner and the outer binary orbits in the triple. Such long term evolution can therefore be modelled using the secular approximation. In this approximation the equations of motion are averaged over the orbital periods of the inner and the outer binary. In the orbit averaged equations only the exchange of angular momentum between the inner and outer orbits is possible, but energy is not exchanged. Hence, such secular evolution can not, by itself, cause changes in the SMA of either of the two orbits.

When the separation between the stars in the inner binary becomes sufficiently small, other physical processes beside pure Newtonian gravitational dynamics come into play. In this work we consider several such effects that can induce additional periapse precession and thereby couple to the KL dynamics and typically tend to suppress it. These additional sources of precession include: apsidal precession due to tidal and rotational bulges, apsidal precession due to general relativity (GR) and the apsidal precession due to tidal dissipation, which is negligible in comparison to the former processes.

The precession rate due to KL mechanism can be either positive or negative. In contrast, the precession rates due to GR and the tidal bulge effect are always positive and tend to promote periapse precession. As a consequence of the interplay between Kozai precession and GR and tidal bulge precession, the maximum eccentricity attainable by the system is lower; at the same time, the critical inclination at which KL evolution becomes significant increases (Eggleton & Kiseleva-Eggleton (2001); Miller & Hamilton (2002); Wu & Murray (2003); Fabrycky & Tremaine (2007), see their Figure 3). Precession rate caused by the rotational bulge may have either positive or negative value. The precession rates due to rotational and tidal bulges raised on both of the stars in the inner binary are parametrized by the tidal Love number k_2, a dimensionless constant that relates the mass of the multipole moment (created by tidal forces on the spherical body) to the gravitational tidal field in which that same body is immersed. k_2 encodes information on the internal structure of the stars[4] and since we consider main sequence stars we adopt $k_2 = 0.028$, a value characteristic for Sun-like stars (Eggleton & Kiseleva-Eggleton 2001; Fabrycky & Tremaine 2007).

When the separation between the stars in the inner binary is of the order of a few stellar radii, tidal dissipation due to a close periapse approach in an eccentric orbit, or due to an asynchronous rotation may play an important role in the dynamical evolution (Mazeh & Shaham 1979; Eggleton & Kiseleva-Eggleton 2001). As the inner binary orbit goes through the phases of high eccentricity the periapse distance may become sufficiently small to induce strong tidal dissipation. The tidal dissipation drains the energy from the orbit, while conserving the angular momentum. As a result the SMA shrinks, which in turn leads to an even stronger dissipation. Since the angular momentum is conserved in this process, it also results in the decrease of orbital eccentricity. Eventually the orbit circularizes at a separation of only a few stellar radii. Tidal dissipation is parametrized by the tidal dissipation factor Q, defined as the ratio between the energy stored in the tidal bulge and the energy dissipated per orbit. We adopt $Q = 10^6$, typically considered to be the characteristic value for sun-like stars (Eggleton & Kiseleva-Eggleton 2001; Fabrycky & Tremaine 2007).

2.2. *Timescales*

The dense stellar environment of a galactic nucleus is prone to dynamical processes which do not typically take place in the field. Such processes can significantly alter the dynamics and eventually the stellar evolution of binaries near the MBH. In this section we briefly review the relevant dynamical processes associated with NSCs hosting MBHs and their timescales. We compare the latter with the secular KL timescales as well as with the timescales associated with the binaries themselves. Additional details on the timescale calculations for the processes considered here can be found in Antonini & Perets (2012).

Let us consider a binary with stellar components of mass m_1 and m_2, orbiting a MBH of mass $M_\bullet$. The eccentricities of the inner and the outer binary are denoted by e_1 and e_{out},

[4] Note that the apsidal precession constant, which is a factor of two smaller than the tidal Love number, but which we do not utilize, is often denoted by k_2 as well.

and the SMAs are denoted by a_1 and a_{out}, respectively. The argument of the periapsis of the inner binary, ω_{in} is defined relative to the line of the ascending nodes, while i is the mutual inclination between the inner and the outer orbit.

Binaries in a dense environment such as the Galactic center are susceptible to evaporation due to dynamical interactions with the surrounding stars. The ratio of the kinetic energy of the field stars to the internal orbital energy of the binary determines whether the binary will evaporate; if this ratio is larger than unity, binaries are expected to evaporate. The evaporation timescale for soft binaries is (Binney & Tremaine 2008):

$$T_{\rm EV} = \frac{M_{\rm b}\sigma}{G16\sqrt{\pi}Ma_1\rho\ln\Lambda} \approx 3\times10^8\left(\frac{2}{\ln\Lambda}\right)\left(\frac{M_b}{2M_\odot}\right)\left(\frac{M_\odot}{M}\right)\left(\frac{\sigma}{100km/s}\right) \times\left(\frac{1AU}{a_1}\right)\left(\frac{\rho_0}{\rho}\right)\ \text{yrs}, \quad (1)$$

where r is the distance from the MBH, ρ the local density of stars, $\ln\Lambda$ the Coulomb logarithm, M the mass of the field stars, $M_{\rm b}=m_1+m_2$, $\sigma=\sqrt{GM_\bullet/r}/(1+\gamma)$ is the local 1D velocity dispersion and γ the slope of the stellar density profile. Hereafter, we adopt $M_\bullet=4\times10^6M_\odot$ (Ghez et al. 2008; Gillessen et al. 2009). We use the values of the normalization parameters $\rho_0=\ 5.2\times10^5[\frac{M_\odot}{\rm pc^3}]$ and $r_0=0.5$ pc typical for a GC-like nucleus and $M=1M_\odot$, and $\gamma=2$ – the slope expected for a dynamically relaxed single-mass population around a MBH.

Binaries orbiting the central MBH with a mutual inclination $i\gtrsim40^\circ$ undergo KL periodic variations of their eccentricity and inclination on a timescale:

$$T_{Kozai}\approx\frac{4}{3\sqrt{G}}\left(\frac{a_{out}}{a_1}\right)^3\frac{M_b^{1/2}}{M_\bullet}a_1^{3/2}(1-e_{out}^2)^{3/2} \approx2.5\times10^6\left(\frac{a_{out}}{0.5\rm pc}\right)^3\left(\frac{1AU}{a_1}\right)^3\left(\frac{M_b}{2M_\odot}\right)^{1/2} \times\left(\frac{4\times10^6M_\odot}{M_\bullet}\right)\left(\frac{a_1}{1AU}\right)^{3/2}(1-e_{out}^2)^{3/2}\ \text{yrs}. \quad (2)$$

Given a simple power law density model, $\rho\sim r^{-\gamma}$, setting $T_{Kozai}\approx T_{\rm EV}$ and $r=a_{out}$ gives the radius below which binaries can undergo at least one KL cycle before they evaporate due to gravitational encounters with surrounding stars:

$$\tilde{r}_{\rm EV}=\left(\frac{6.8\times10^{-4}}{\left([1+\gamma]\rho_0r_0^\gamma\right)^2}\frac{a_1}{\ln\Lambda^2}\left(\frac{M_\bullet}{M_b}\right)^3\left(\frac{M_b}{M}\right)^2 \times\frac{M_b^2}{(1-e_{out}^2)^3}\right)^{1/(7-2\gamma)} \approx\frac{0.885}{(1-e_{out}^2)}\left(\frac{2M_\odot}{4\times10^6M_\odot}\frac{M_\bullet}{M_b}\right)\left(\frac{1}{2}\frac{M_b}{M_\odot}\right)^{4/3} \times\left(\frac{4}{\ln\Lambda^2}\frac{a_1}{\rm AU}\right)^{1/3}\ \text{pc}, \quad (3)$$

For $a_{out}\gtrsim\tilde{r}_{\rm EV}$ the binary evaporates before completing one KL cycle. For realistic values of the adopted parameters, $\tilde{r}_{\rm EV}$ is comparable to the extent of the disk of young stars at the Galactic center and can be of order the SgrA* influence radius. However, at radii smaller than this critical radius KL cycles are detuned by fast relativistic precession of the inner binary orbit. It can be shown that general relativistic precession in the inner binary suppresses the KL oscillations at radii larger than (Holman et al. 1997; Blaes et al. 2002):

$$\tilde{r}_{\rm SC}=0.02\left(\frac{a_1}{\rm AU}\right)^{4/3}\left(\frac{M_b}{2M_\odot}\right)^{-2/3} \times\left(\frac{M_\bullet}{4\times10^6{\rm M}_\odot}\right)^{1/3}\left(\frac{1-e_1^2}{1-e_{out}^2}\right)^{1/2}\ \text{pc}\ . \quad (4)$$

For $a_{out}\gtrsim\tilde{r}_{\rm SC}$ KL cycles are quenched by rapid Schwarzschild apsidal precession. This preliminary analysis shows that the MBH induced KL cycles on GC binaries might be only important inside a tenth or possibly up to a few tenths of a parsec from the center (where the exact distance depends on the density profile model and orbital eccentricity). The maximum eccentricity such binaries can attain is not largely affected by relativistic precession while, at the same time, they can perform several KL oscillations before being dissociated by encounters with field stars or before their components evolve to leave the main sequence.

3. INITIAL CONDITIONS AND METHODOLOGY

On the basis of the previous discussion, we concluded that only binaries on orbits passing relatively close to the MBH can be significantly affected by KL oscillations. Therefore, in the following we only consider binaries within a galactocentric radius $\lesssim0.5$ pc; this radius also corresponds roughly to the outer extent of the young stellar disk in the central parsec of the GC. The inner parsec of the Galaxy contains two distinct populations of young stars. One population, mainly O giants/supergiants and WR stars, is observed to have a disk-like structure extending from 0.5 pc inward to within 0.05 pc of the MBH (Bartko et al. 2009; Lu et al. 2013). A second population of young stars consists of longer lived B-type main sequence stars that appear more isotropically distributed (Bartko et al. 2010; Perets & Gualandris 2010). The B-stars with projected radii of less than one arcsecond are usually referred to as the "S-stars". We consider binaries originating from both the stellar disk and the stellar cusp surrounding it. The total number of integrated binaries is 1367 for those originating from the disk, and 1670 for those originating from the cusp. In Section 3.1 we describe the choice of parameters for the binaries, while in Section 3.2 we discuss the choice of parameters for the orbits of the binaries around the MBH, i.e. the distribution of the outer orbits of the MBH+binary triples.

3.1. *Inner binary parameters*

Binaries originating from the stellar disk are assumed to be relatively massive; the masses of primary stars, m_1, are drawn from a top heavy initial mass function (IMF) with a power-law slope of $\alpha_{DISK}=1.7$ (Lu et al. 2013). The primaries of binaries originating from the stellar cusp are assumed to follow a Salpeter IMF with slope of $\alpha_{CUSP}=2.35$ (Salpeter 1955). We set the mass of the secondary stars m_2 to be equal to m_1 in 40% of the cases, while the others are chosen by selecting the mass ratio $q_{in}=m_2/m_1$ uniformly between 0 and 1. The

TABLE 1. Inner binary parameters

Symbol	Definition	Distribution
m_1	primary mass	IMF with α_{DISK} = 1.7 and α_{CUSP} = 2.35
m_2	secondary mass	40% twins, 60% (m_2/m_1) uniform in (0,1)
a_1	Inner binary semimajor axis	lognormal with $< logP(d) >$= 4.8 and $\sigma(d)$ = 2.8
$e_{1,0}$	Inner binary initial eccentricity	thermal, $e_{in,0} < 0.9$
i_{init}	Initial mutual inclination	uniform in cos(i)
$\omega_{in,0}$	Initial argument of periastron	uniform
Ω_{in}	Longitude of ascending node	uniform
$R_{1,2}$	stellar radius	$R_{1,2} = (m_{1,2}/M_\odot)^{0.75} R_\odot$
$r_{p,in}$	inner binary periapse	$r_{p,in} \geq 5(R_1+R_2)$
k_2	Tidal Love number	0.028
Q	Tidal dissipation factor	10^6

stars are initially taken as MS stars with appropriate MS radii, $R_{1,2} = R_\odot (m_{1,2}/M_\odot)^{0.75}$. The initial orbital period of the (inner stellar) binaries is chosen from a log-normal distribution following Duquennoy & Mayor (1991), with $\langle logP(days) \rangle$ = 4.8 and $\sigma_{logP(days)}$ = 2.8. A thermal distribution for the inner binary eccentricity is assumed. The initial mutual inclination between the binary orbit and the orbit around the SMBH is uniform in cos$i$. The argument of periapse and the longitude of the ascending node are uniformly distributed. For tidal Love number, tidal dissipation factor, and moment of inertia of the binary components we use values of $k_2 = 0.028$, $Q = 10^6$ and $I_{1,2} = 0.08 m_{1,2} R_{1,2}^2$, respectively, which are typical for Sun-like stars (Eggleton & Kiseleva-Eggleton 2001). The initial spin periods of the binary components is set to 10 days and the spin angular momentum is aligned with the orbital angular momentum of the binary. We only integrate systems for which the initial inner binary periapse is larger than $5 \times (R_1 + R_2)$, to assure that the outcome of the integration is indeed due to KL mechanism and not pure tidal dissipation. Table 1 summarizes our choice of parameters for the inner binary orbits.

3.2. *Outer binary parameters*

To model the mass density of stars in an NSC similar to the GC we use a power-law density profile:

$$\rho(r) = \rho_0 \left(\frac{r}{r_0}\right)^{-\gamma} \left[1 + \left(\frac{r}{r_0}\right)^2\right]^{(\gamma-1.8)/2}, \quad (5)$$

where here γ is the slope of the inner density profile. We adopt $r_0 = 0.5\,$pc and $\rho_0 = 5.2 \times 10^5 [\frac{M_\odot}{\rm pc^3}]$, which give a good fit to the observed spatial density at the GC outside the core (normalized at 1 pc; (Schödel et al. 2009)). All timescales considered are computed for two models for the inner density profile: (1) a shallow power-law slope, $\gamma = 0.5$, representing the observed distribution of stars at the GC (Buchholz et al. 2009; Do et al. 2009; Bartko et al. 2010); (2) a steep power-law slope, $\gamma \approx 2$, corresponding to a nearly relaxed configuration of stars in a potential dominated by a MBH (Alexander 2005). The outer binary parameters depend on the origin of the binaries; the stellar disk, that extends from $\sim 0.04\,$pc to $\sim 4\,$pc, or the stellar cusp. For each set of binaries we compute the binary evaporation time in this collisional environment considering both the shallow density profile model and the the steep cusp density profile mentioned above. For binaries originating from the stellar disk we draw the SMAs of the outer binaries (i.e, for the orbit around the MBH) from the distribution $dN(a)/da \sim a_{out}^{-1}$ following Lu et al. (2009) while for the eccentricity of the outer orbit we adopt the double-peaked distribution from Bartko et al. (2009) which has two maxima at $e_{out} \sim 0.35$ and $e_{out} \sim 0.95$.

For binaries originating from the stellar cusp we sampled the orbital elements of the binary around the MBH from the following distribution:

$$N(a, e^2) = N_0 a^{2-\gamma} da de^2, \quad (6)$$

i.e. assuming a steady-state phase-space distribution for an isotropic cusp in the neighbourhood of a dominating point mass potential. Therefore, the SMAs are drawn from a $dN/da \sim a^{2-\gamma}$ distribution, while the eccentricity distribution of the binary orbit around the MBH is taken to be thermal. The background cusp determining the binary evaporation time was modelled using the density profile of equation 5.

For the shallow cusp density profile, ($\gamma = 0.5$), we use equation 5 where we set $r_0 = 0.5\,$pc and $\rho_0 = 5.2 \times 10^5 [\frac{M_\odot}{\rm pc^3}]$. We compute the evaporation time scale of the binary systems assuming stellar mass perturbers for the $\gamma = 0.5$ model. In the steep cusp density profile model we compute the evaporation time taking into account both stellar and BH perturbers. The combined density profile corresponds to a mass segregated cusp near a MBH :

$$\rho(r) = \rho_\star(r) + \rho_{BH,0} \left(\frac{r}{0.5\,\rm pc}\right)^{-2}, \quad (7)$$

where $\rho_{BH,0} = 10^4 [\frac{M_\odot}{\rm pc^3}]$ and $\rho_\star$ corresponds to the stellar density profile given by equation 5 with $\gamma = 1.5$, the density profile slope of the main sequence star population in the quasi-steady state multimass models of Hopman & Alexander (2006).

TABLE 2. Parameters determined by the model

Symbol	Disk, $\gamma = 1.5$	Disk, $\gamma = 0.5$
a_{out}	$\frac{dN(a)}{da} \sim a_{out}^{-1}$ (Lu et. al 2009)	$\frac{dN(a)}{da} \sim a_{out}^{-1}$ (Lu et. al 2009)
e_{out}	from Bartko et. al 2009.	from Bartko et. al 2009
$\rho_\star [\frac{M_\odot}{pc^3}]$	$5.2 \times 10^5 (\frac{a_{out}}{0.5pc})^{-1.5}$	$5.2 \times 10^5 (\frac{a_{out}}{0.5pc})^{-0.5}$
Symbol	Cusp, $\gamma = 1.5$	Cusp, $\gamma = 0.5$
a_{out}	$\frac{dN(a)}{da} \sim a_{out}^{0.5}$	$\frac{dN(a)}{da} \sim a_{out}^{1.5}$
e_{out}	thermal	thermal
$\rho_\star [\frac{M_\odot}{pc^3}]$	$5.2 \times 10^5 (\frac{a_{out}}{0.5pc})^{-1.5}$	$5.2 \times 10^5 (\frac{a_{out}}{0.5pc})^{-0.5}$
$\rho_{BH} [\frac{M_\odot}{pc^3}]$	$10^4 (\frac{r}{0.5pc})^{-2}$	
$r_{p,out}$	$r_{p,out} \geq 4 \times r_{bt}$	$r_{p,out} \geq 4 \times r_{bt}$

3.3. *Dynamical model: Secular KL evolution with tidal friction (KCTF) in octupole approximation*

We treat the gravitational effects of the third body in the octupole approximation, where we derive the equations of motion from the double-averaged Hamiltonian. In other words we average over the orbital periods of both the inner binary and the binary orbit around the MBH, and retain terms up to (a_1/a_{out}) to 3^{rd} order. Beside the perturbations due to the presence of the third body via KL mechanism, we include the following dynamical effects:

- periastron advance due to general relativity in the inner binary;
- periastron advance arising from quadrupole distortions of the inner binary stars due to both tides and rotation;
- orbital decay due to tidal dissipation in the inner binary stars.

The equations used in our model are those of Ford et al. (2000) and Blaes et al. (2002) for the octupole terms, combined with equations from Prodan & Murray (2012) for tidal effects on both stars in the binary. Since we integrate only systems for which $r_{p,out} > 4 \times r_{bt}$, where $r_{bt} \sim \left(\frac{M_\bullet}{m_1+m_2}\right)^{1/3} a_1$, the secular approximation is justified. In this parameter regime the results of the octupole integration are in good agreement with the results of direct N-body integration (Antonini et al. 2010; Antonini & Perets 2012). During the integration of the binaries evolution we regard an event as a "merger" when one of the binary members starts overflowing it's Roche lobe, which for MS stars occurs at $r_{p,in} \approx (R_1 + R_2)$. Our code does not treat mass transfer or mass loss. The stopping condition for the integration are:

- binary "mergers" occurred, $r_{p,in} \approx (R_1 + R_2)$ or one of the binary members starts overflowing its Roche lobe;
- binary has evaporated due to dynamical interactions with field stars, $t \approx T_{EV}$;
- one or both components reached the end of their main sequence lifetime $t \approx T_{MS}$;
- the maximum integration time for the binaries originating from the stellar disk is $T_{max} = 10^7$ yr which corresponds approximately to the lifetime of the stellar disk; while the maximum integration time for the binaries originating from the cusp is set to $T_{max} = 10^{10}$ yr.

3.4. *Binary stellar evolution*

We account for binary mergers due to KCTF during the MS lifetime of binary components in the dynamical evolution phase discussed above. However, KCTF evolution could significantly affect the orbital evolution of a binary without leading to a merger during the MS phase, and therefore strongly impact its long term evolution beyond the MS. In order to explore such possible effects, we follow the binary stellar evolution of the non-merged binaries from the KCTF stage. We use a simplified approach, in which we take the final orbital configuration of all non-merged binaries from the KCTF stage, and then follow their evolution using the binary stellar evolution population synthesis code BSE developed by Hurley et al. (2000). In order to explore the importance of the role that KCTF plays during the MS phase on the binary stellar evolution, we also consider the evolution of the same binaries using their initial configuration, before any KCTF evolution occurred. In both cases we initialize the systems with zero age MS components. Finally, we compare the results of the stellar evolution of both groups.

Such comparison provides a fraction of systems that are significantly affected by KCTF, and are defined as concurring with at least one of the following:

1. The stellar type (as defined in the BSE code; e.g. a WD vs. a red-giant) of at least one of the stellar components in the KCTF evolved binary differs from its corresponding non-KCTF evolved binary.
2. At least one of the binary components mass differs from its corresponding non-KCTF evolved binary by more than 5% (the fraction is with respect to the more massive relevant star, either from the KCTF or non-KCTF evolved case).
3. The binary orbital period changed by at least 10 %.

The change in the eccentricity of the inner binary is a natural consequence of KL evolution, but just on its own it might not notably impact the binary evolution. Therefore, we do not consider this change in eccentricity by itself as a driver defining a significant difference in the evolution of the two groups.

There are two main caveats with this simplistic approach. First, during the BSE phase we do not account for any KCTF evolution, while such effects could be significant and further affect the binary evolution; it is therefore likely that our calculated fractions of systems affected by the combined KCTF and further BSE are only underestimates for the more significant actual impact. Second, the time during which the KCTF evolution was followed is not accounted in the later BSE, i.e. the KCTF binaries are assumed to be zero age MS binaries, with only their orbital parameters changed due to KCTF. For these reasons the detailed types of binary systems produced in the KCTF+BSE (e.g. X-ray binaries, CVs etc.) are not discussed; rather, only the overall fractions of systems in which early KCTF evolution gave rise to significant difference in the later BSE are calculated, providing a first order estimate of the effects discussed in this paper. More detailed results of population synthesis of binaries near MBHs is beyond the scope of this paper, and would require a triple stellar evolution code, in which binary stellar evolution and the triple system dynamics are inherently coupled (See Perets & Kratter 2012; Hamers et al. 2013, for initial steps in this direction).

4. RESULTS

4.1. *KCTF evolution*

In this section we present the results of our numerical model for the secular evolution of the binaries around the MBH. As described in the previous section, we consider binaries originating from both the stellar disk and the stellar cusp. In both cases we model the background cusp considering either the shallow or the steep density profile models in order to determine the relevant evaporation timescales. Details on how we

generate the initial conditions are found in Section 3. The outcomes of such evolution can be divided in following categories:

- "mergers"– one of the binary components starts overflowing its Roche lobe or they physically collide ($r_{p,in} \approx (R_1+R_2)$). In the case of main sequence stars these two conditions are almost equivalents since main sequence stars need to be almost touching each other in order to start Roche lobe overflow.
- Evaporated binaries – the two components of the binary are no longer bound together due to the interaction with the field stars. Whether the binary will evaporate or not strongly depends on the assumed density profile of the background cusp and the binary SMA. For example, using a steeper density profile increases the central density of background stars, reduces the binaries evaporation times and in turn increases the percentage of evaporated systems.
- Tidally affected binaries – as long as the perturbation from the MBH effectively excites the eccentricity, the binary SMA may suffer dramatic shrinkage due to tidal dissipation. As the binary becomes tighter the probability for its evaporation decreases (see equation 1).

Figs. 1 and 2 show the histograms for the binary evolution outcomes for both the stellar-disk binaries and the cusp binaries, and for both the shallow and the steep density profile models. We find that $\sim 3\%$ of the stellar-disk binaries experience “mergers" while on the MS. The same is true for $\sim 1\%$ of the steep cusp binaries and $\sim 0.25\%$ of the shallow cusp model binaries (see Table 3 as well). The majority of “mergers" occur for initially highly inclined orbits and at the first maximum in the KL cycle. The merging systems are not very sensitive to evaporation precesses as the KL timescale for most of these systems is orders of magnitude shorter than their evaporation time (see Section 2.2). Due to the larger number of objects closer to the MBH, where $a_{out} \lesssim \tilde{r}_{\rm SC}$, the binaries in the steep cusp model can in average achieve higher eccentricities and are more likely to merge than binaries in the shallow cusp model. As a consequence of this the number of mergers in the steep cusp model is about four times larger than in the core model.

The difference in the percentage of "mergers" between stellar-disk and cusp binaries is due to the selected IMF. As mentioned before, the mass of the binary components of the stellar-disk binaries is drawn from a top heavy IMF. Therefore, the ratio of their physical size to the separation is larger than that of the less massive cusp binaries (following a Salpeter IMF), resulting in a higher "merger" rate. The observed peak at high inclinations in the distribution of surviving stellar-disk binaries is due to those binaries that shrank significantly due to KCTF. Such evolution also increases their evaporation time beyond the lifetime of the stellar disk (10^7 yr). The same effect produces a similar peak at high inclinations for cusp binaries followed until they evolved off the main sequence. The shape of the density profile determines the percentage of evaporated binaries; when a steep density profile model is assumed, the number/percentage of evaporated systems is higher, as expected. On that account, at the end of the calculated dynamical evolution, after 10^7 yr, the distributions of the surviving systems in the shallow and steep density profile models is distinctively different.

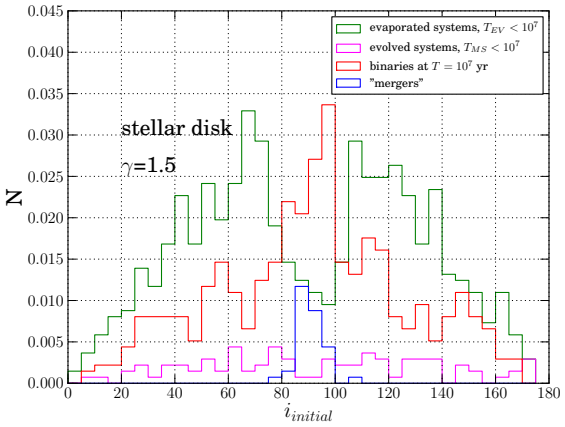

FIG. 1.— Histogram of the initial inclination for the binaries in the stellar disk for $\gamma = 1.5$. Approximately 3% of the systems are likely to merge while on the main sequence. All "mergers" on the main sequence occur in systems with high mutual inclinations and already during the first Kozai–Lidov cycle. The percentage of "mergers" is not affected by the choice of a density profile, but the number of systems that evaporate is higher when a steep density profile is considered, as expected.

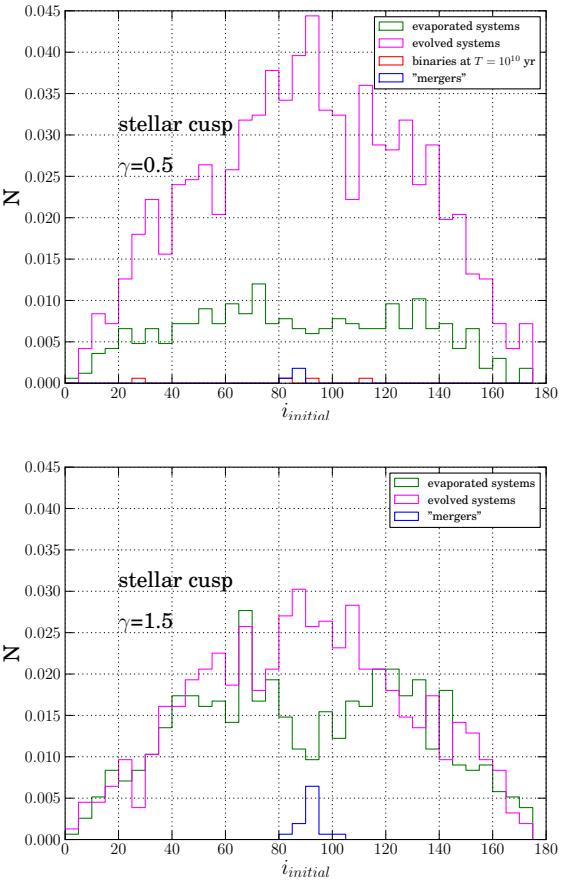

FIG. 2.— Histogram of the initial inclination of cusp binaries: left panel shows results for $\gamma = 0.5$ and the right panel shows results for $\gamma = 1.5$. Approximately $2-3\%$ of the systems are likely to merge while on the main sequence. Similar to the case of stellar-disk binaries, all "mergers" occur for high mutual inclinations and already on the first Kozai–Lidov cycle. Again, the choice of the density profile does not affect the percentage of "mergers" and the number of evaporated systems is higher in the steep density profile model case, as expected.

Fig. 3 shows the dependence of the ratio of the final SMA the initial SMA of the inner binary on the closest approach to the MBH, scaled to the tidal disruption radius; ($a_{final}/a_{initial}$ vs. $r_{p,out}/r_{bt}$). The stellar-disk model clearly demonstrates that for the majority of "mergers" tidal dissipation is not important. In other words, the KL timescale is much shorter than the tidal dissipation timescale due to the strong Kozai torque ($a_{final}/a_{initial} \sim 1$), and the same is true for the stellar cusp model. Since the period of KL cycles strongly depends on the separation of the perturber ($T_{Kozai} \sim a_{out}^3$), the region where tidal dissipation becomes important is $r_{p,out} < 100 \times r_{bt}$. For many binaries in this region, Kozai torque is strong enough to induce significant eccentricity oscillations but the eccentricity does not reach sufficiently high values to result in a "merger". Instead, during the high eccentricity phase of a KL cycle, the periapse separation of the binary becomes small enough for tides to become important to the evolution. As seen in Figure 4 the systems that experience dramatic tidal evolution are those in the KL high inclination regime. Due to the energy drained by tidal dissipation at periapse passage, their SMA significantly shrinks. After these stars evolve off the MS, their radii expand due to stellar evolution which, in principle, could result in an even stronger tidal effects. Eventually, such combination of KL cycles with tidal friction may lead to the binary coalescence or strong binary interaction during the post-MS phase.

The shrinkage of the SMA of the inner binary due to KCTF becomes important when it comes to the survival of binaries in the environment of the GC. Our calculations demonstrate that the survival rate of the binaries is $\sim 10\%$ higher than in the case where KL evolution is neglected (due to the binary hardening as a result of KCTF-induced SMA shrinkage).

Figs. 5 and 6 depict the dependence of the ratio of the final SMA to the initial SMA of the inner binary, on the outer SMA (separation of the inner binary from the MBH) for the stellar-disk and cusp binaries, and for both the shallow and the steep density profile models. As already emphasized, both figures demonstrate that tidal dissipation is not a main driver for the occurrence of "mergers". Figure 5 shows that tidal dissipation significantly impacts systems within a distance of ~ 0.1 pc from the MBH. Such systems shrink and harden due to KCTF and can survive stellar scatterings longer; (T_{EV} becomes longer as a_{in} shrinks). This process can, in principle, affect the observed period distribution of stars in the stellar-disk. Fig. 6 shows that all of the tidally affected cusp binary systems reside beyond ~ 0.1 pc from the MBH. A number of these system has periapse distance of only few stellar radii i.e. systems for which $R_{SUM} < r_p \leq 2 \times R_{SUM}$. The difference in the location of regions containing tidally affected systems in the disk and in the cusp lies in the choice of initial distribution of a_{out} (see Table 2).

Figs. 7 and 8 show the cumulative distribution of "mergers", evaporated systems, evolved systems and surviving binaries for both stellar-disk and cusp binaries. As seen in Fig. 8, the majority of mergers occur at early times during the first Kozai cycle. We found that the fraction of mergers is sensitively higher if the binaries originate in a stellar disk characterized by a top heavy initial mass function. In this latter case the ratio of the stars physical size to their separation in a binary is larger than that of the less massive cusp binaries, which increases the chance for a close stellar interaction. The density profile is an important factor in determining the percentage of evaporated systems which, as expected, is significantly higher in the case of a steep density profile ($\gamma = 1.5$) model.

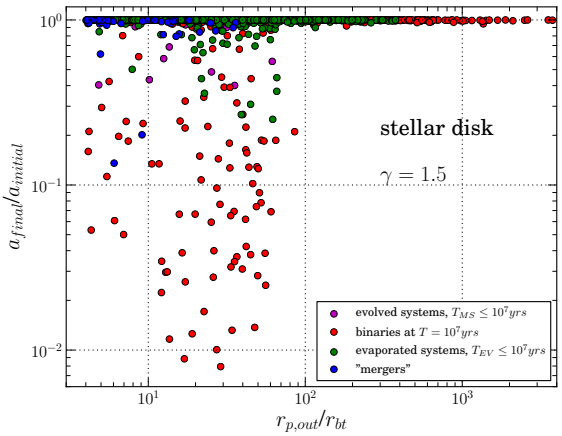

FIG. 3.— $a_{final}/a_{initial}$ vs. $r_{p,out}/r_{bt}$ for the stellar disk: $\gamma = 0.5$ (upper panel) and $\gamma = 1.5$ (lower panel). Both choices of γ demonstrate that for the majority of "mergers" tidal dissipation is not relevant ($a_{final}/a_{initial} \sim 1$). The region where tidal dissipation is important is $r_{p,out} < 100 \times r_{bt}$. Once the stars leave the main sequence, their radius expands due to stellar evolution, and tidal effects may become even stronger. Such a combination of tidal effects and Kozai–Lidov cycles could lead to post main sequence coalescence/ strong binary interaction.

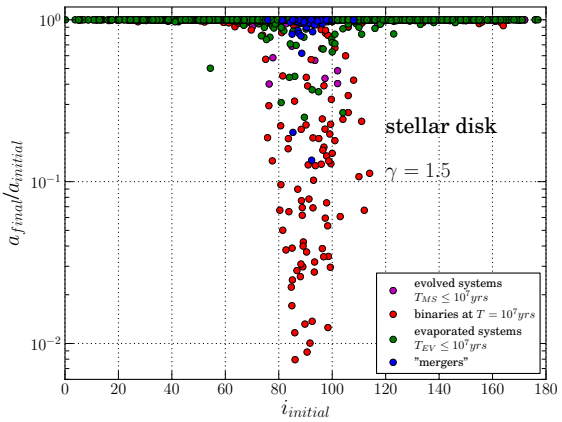

FIG. 4.— $a_{final}/a_{initial}$ vs. $i_{initial}$ for the stellar disk for $\gamma = 1.5$. For the majority of "mergers" tidal dissipation is not relevant. Tidal dissipation is important for inclinations in the range $70^o \lesssim i_{initial} \lesssim 110^o$. Similar results are obtained for the cusp model.

TABLE 3. Results of simulations

fraction of systems	Disk $\gamma = 1.5$	Disk $\gamma = 0.5$	Cusp $\gamma = 1.5$	Cusp $\gamma = 0.5$
"mergers"	0.03	0.03	0.01	0.0025
evaporated	0.554	0.043	0.45	0.213
evolved	0.063	0.073	0.54	0.782
binaries	0.353	0.85	0	0.0025
integration T_{max} [yr]	10^7	10^7	10^{10}	10^{10}

All our integrations and their outcomes are summarized in Table 3.

4.2. *Post KCTF Binary stellar evolution*

TABLE 4: Fraction of evolved binary systems significantly affected by Kozai-Lidov and tidal friction evolution.

Cusp Models	**Time (Myrs)**								
Cusp - γ = 0.5	5	10	50	100	500	1000	5000	10000	12000
Stellar type change 1	0	0.01	0.03	0.04	0.07	0.08	0.10	0.11	0.11
Stellar type change 2	0	0.01	0.04	0.06	0.10	0.11	0.12	0.13	0.13
Period change	0.05	0.07	0.10	0.10	0.13	0.13	0.14	0.14	0.14
Mass change 1	0	0	0.01	0.03	0.06	0.09	0.23	0.27	0.28
Mass change 2	0	0.02	0.12	0.17	0.28	0.34	0.48	0.50	0.51
Total evolutionary changes	0.05	0.08	0.20	0.26	0.39	0.47	0.66	0.71	0.72

Cusp - γ = 1.5									
Stellar type change 1	0	0.01	0.04	0.06	0.10	0.10	0.12	0.13	0.13
Stellar type change 2	0	0.02	0.04	0.07	0.11	0.13	0.14	0.15	0.15
Period change	0.06	0.07	0.10	0.13	0.15	0.15	0.16	0.17	0.18
Mass change 1	0	0	0.02	0.03	0.10	0.15	0.28	0.31	0.32
Mass change 2	0	0.03	0.15	0.22	0.38	0.46	0.57	0.58	0.58
Total evolutionary changes	0.06	0.09	0.24	0.32	0.52	0.61	0.77	0.80	0.80

Disk Models	**Time (Myrs)**								
Disk - γ = 0.5	5	10	50	100	500	1000	5000	10000	12000
Stellar type change 1	0.01	0.08	0.08	0.07	0.07	0.07	0.08	0.08	0.08
Stellar type change 2	0.04	0.14	0.14	0.13	0.13	0.13	0.14	0.14	0.14
Period change	0.05	0.18	0.20	0.20	0.20	0.20	0.21	0.21	0.21
Mass change 1	0	0.01	0.01	0.02	0.02	0.02	0.04	0.04	0.04
Mass change 2	0.03	0.23	0.26	0.26	0.26	0.26	0.26	0.26	0.26
Total evolutionary changes	0.06	0.33	0.38	0.38	0.38	0.38	0.40	0.40	0.40

Cusp - γ = 1.5									
Stellar type change 1	0.01	0.08	0.15	0.15	0.15	0.13	0.15	0.16	0.16
Stellar type change 2	0.04	0.15	0.19	0.19	0.19	0.18	0.19	0.20	0.20
Period change	0.06	0.18	0.19	0.19	0.19	0.18	0.19	0.19	0.19
Mass change 1	0	0	0.08	0.08	0.08	0.08	0.10	0.11	0.11
Mass change 2	0.03	0.26	0.27	0.27	0.27	0.27	0.27	0.27	0.27
Total evolutionary changes	0.07	0.37	0.41	0.41	0.41	0.41	0.44	0.44	0.44

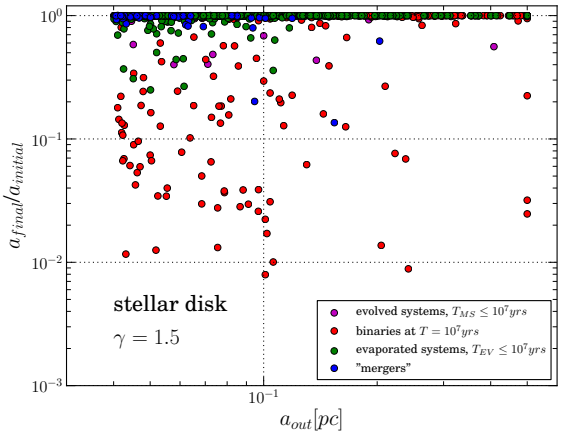

FIG. 5.— $a_{final}/a_{initial}$ vs. a_{out} for the stellar disk and a steep density profile model (γ = 1.5). The majority of "mergers" occur within 0.1 pc off the MBH and are not driven by tidal dissipation ($a_{final}/a_{initial} \sim 1$). Systems in this region that did not coalesce were strongly affected by KCTF evolution.

Once the binaries go off the main sequence and become giants, their radius will significantly expand. The high eccentricities induced via the KL mechanism, combined with such an expansion in the size of each inner binary star, could lead to efficient production of coalescing/strongly-interacting post-MS binaries. Accounting for the effects of the KCTF on the long term stellar evolution of the binaries is therefore an important step.

In Table 4 we show the fraction of binary systems in which stellar evolution was significantly affected by their earlier KCTF evolution. We evolve 1304 binaries with γ = 0.5 and 846 binaries with γ = 1.5 originating from the cusp; and 106 binaries with γ = 0.5 and 89 binaries with γ = 1.5 originating from the disk. In the cusp models the stellar evolution of the majority of the binaries is significantly affected; rising from 45-60 % after one Gyr and up to 70-80 % after 10 Gyrs of evolution. In the disk models KCTF significantly affected a large fraction (30-40 %) of the binaries already during the first 10 Myrs of evolution, i.e. it should have affected the observed stellar population in the GC stellar-disk which is of comparable age. Also shown is the the later evolution of stellar-disk binaries beyond 10 Myrs (which could be relevant to past epochs of disk star formation), though most of the effects already arise by 10 Myrs.

The time t = 0 in table 4 corresponds to the beginning of the of the evolutionary MS evolution (i.e. all binary components begin as ZAMS stars). However, note that the KCTF binaries begin their evolution with the orbital parameters AFTER the KCTF evolution. In other words their evolutionary time is reset to zero, while the orbital parameters are taken after the KCTF evolution on the MS. This inconsistency does not affect the results significantly, as the main KCTF evolution occur on time scales which are (typically) much shorter than the evolutionary timescales; in particular letting the binaries evolve with the additional MS time, but with their new post-KCTF orbits make little affect on their evolution compared with their post-MS evolution.

Note that in some cases the fractions of KCTF-affected binaries slightly drop at some evolutionary time compared to earlier times. This can arise, for example, when a secondary component in a post-KCTF binary evolves faster than the corresponding star in the binary evolved in isolation (non-

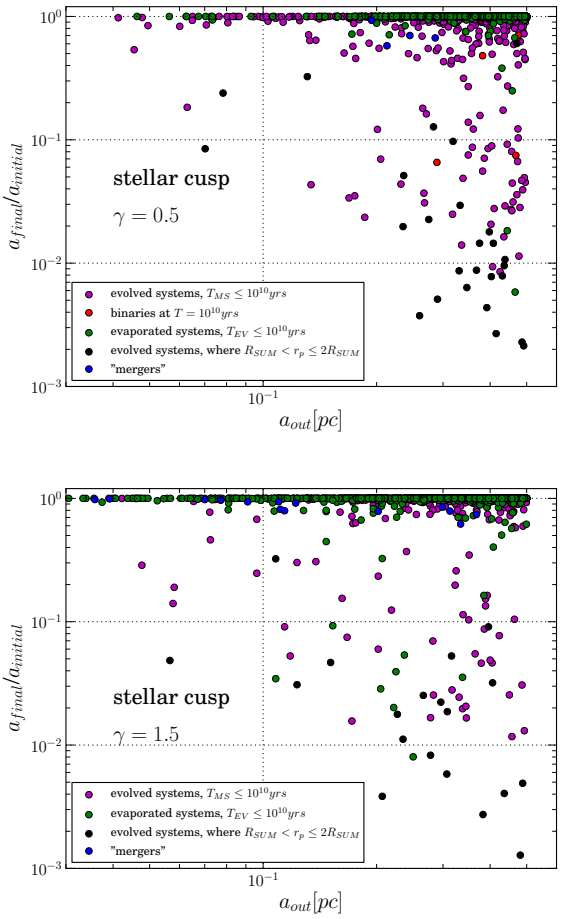

FIG. 6.— $a_{final}/a_{initial}$ vs. a_{out} for the stellar cusp and a the two density profile models (γ = 0.5) (upper panel) and γ = 1.5 (lower panel). Again, both models demonstrate that the majority of "mergers" are not driven by tidal dissipation ($a_{final}/a_{initial} \sim 1$), and KCTF becomes important for systems in the central 0.1 pc region.

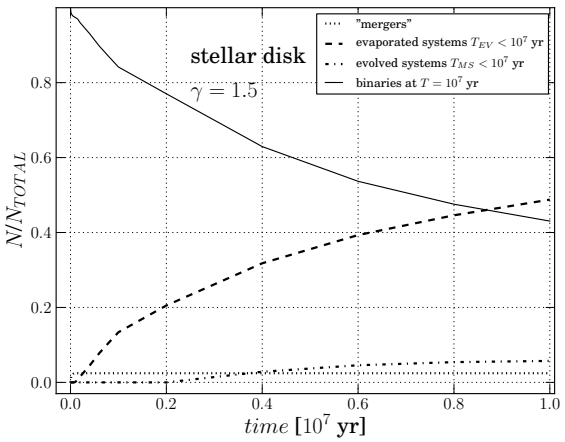

FIG. 7.— Cumulative distribution of '"mergers", evaporated systems, evolved systems and surviving binaries for the binaries in the stellar disk with γ = 1.5.

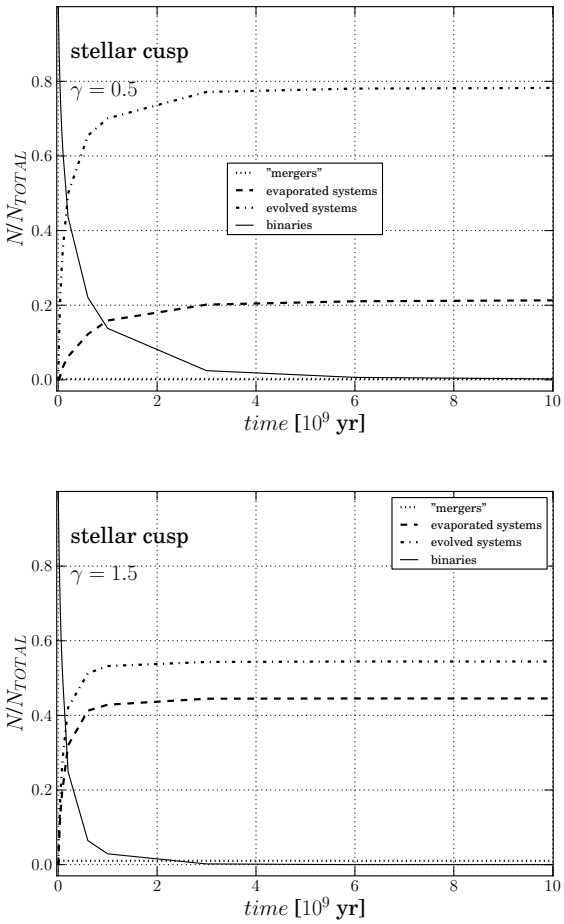

FIG. 8.— Cumulative distribution of "mergers", evaporated systems, evolved systems and surviving binaries for the binaries in the stellar cusp and the density profile models γ = 0.5 (upper panel) and γ = 1.5 (lower panel). The fraction of "mergers" is not affected by the choice of the slope of the density profile while the number of evaporated systems clearly is. Steeper density profile leads to higher fraction of evaporated systems.

KCTF). Such a star may change its stellar type, e.g. it accreted mass, became more massive and evolved faster to become a WD at some stage. The same component in this example may also evolve later-on to become a WD. For this reason the systems may be counted as differing (in terms of the stellar type of the secondary component) at an early stage when the star is a WD in the post-KCTF case, but its corresponding non-KCTF evolved star is still a red-giant. At the later stage, when the this non-KCTF case also evolves to a WD, the stars are counted as similar in terms of their stellar type, but may be counted as differing in their masses. Therefore, once we account for all possible changes included (stellar type, mass and period)[5], the overall fraction of affected KCTF-binaries is a monotonically rising function, and the analysis captures the overall magnitude of changes due to the early KCTF evolution.

4.3. *N-body integration*

[5] a post-KCTF system is counted as differing from its corresponding non-KCTF one if at least one of these elements change, and is not counted twice if more than one change is observed; hence the "total evolutionary changes" row in Table 4, is not a simple sum of the rows above

TABLE 5. Inner binary parameters in N-body runs

Symbol	Definition	Distribution
$m_{1,2}$	stellar mass	IMF with α = 1.7
a_1	Inner binary semimajor axis	lognormal with $< logP(d) >$= 4.8 and $\sigma(d)$ = 2.8
$e_{1,0}$	Inner binary initial eccentricity	thermal
i_{init}	Initial mutual inclination	uniform in (75^o, 105^o)
$R_{1,2}$	stellar radius	$R_{1,2} = (m_{1,2}/M_\odot)^{0.75} R_\odot$
$r_{p,out}$, Set 1	external orbit periapse	$5 \times r_{bt}$
$r_{p,out}$, Set 2	external orbit periapse	uniform in $(0, 10 \times r_{bt})$
$r_{apo,out}$	external orbit apoapse	0.03 pc
k_2	Tidal Love number	0.028
Q	Tidal dissipation factor	10^6

The orbit average approximation used in 4.1 is based on the assumption that the binary angular momentum, $\ell_1 = \sqrt{1-e_1^2}$, changes on timescales that are longer than both inner and outer binary orbital periods. As discussed below, the fact that ℓ_1 can change on a timescale short compared to the inner binary period has special implications for our study. The condition that the binary angular momentum changes by order of itself between two consecutive periapsis passages can be expressed in terms of the system SMAs and eccentricities as (Antonini et al. 2014):

$$\sqrt{1-e_1} \lesssim 5\pi \frac{M_\bullet}{M_b} \left[\frac{a_1}{a_{out}(1-e_{out})} \right]^3 . \quad (8)$$

If the binary eccentricity satisfies this condition than the orbit can evolve and reach $e_1 \sim 1$, i.e. a colliding trajectory, before post–Newtonian (PN) and tidal terms can limit the maximum eccentricity attainable during a KL cycle. Thus, we expect some systems that do not merge when using the double averaged approach, to merge when they are evolved through direct integration of the equations of motion.

We note that oscillations occurring on the orbital timescale of the outer orbit can be also important to the evolution (Antognini et al. 2014). However, the condition given by equation (8) turns out to be the most relevant for our study given that the majority of merging systems can collide only if they experience a clean collision, i.e., a collision where dissipative and non dissipative tidal and (PN) terms do not play an important role. More specifically, the condition for such an event requires that changes in the binary angular momentum occurring over the orbital period of the binary are of the same order of, or larger than the angular momentum associated with the scale at which other dynamical processes (e.g., tidal dissipation or GR precession) can affect the evolution. For example, considering a conservative dissipation scale $\tilde{r} = 2(R_1+R_2)$, we find (Antonini et al. 2014):

$$\frac{r_{p,out}}{r_{bt}} \lesssim 10 \times \left(\frac{a_1}{\mathrm{AU}} \frac{10^{11}\mathrm{cm}}{\tilde{r}} \right)^{1/6} . \quad (9)$$

In this region of parameter space, where ℓ_1 can change on the timescale of order of binary period, the orbit average approximation cannot accurately describe the binary dynamics.

In order to determine the likelihood for a stellar merger within the region of parameter space where the orbit average technique is less accurate, we carried out a number of direct integration of three-body systems. These consist of binaries with orbital periapsis distance to the MBH $a_{out}(1-e_{out})/ \lesssim 10 r_{bt}$. It is from these systems, which experience a relatively close approach to the MBH, that we expect the largest number of mergers, as well as a larger discrepancy between the results of the three-body integration and the predictions of the orbit average equations (e.g., equation 9).

The triple systems were evolved using the high accuracy integrator AR-CHAIN (Mikkola & Merritt 2008) which includes PN corrections up to order 2.5; to these we added terms corresponding to apsidal precession due to tidal bulges and tidal dissipation. We model tidal effects using the formulation given in equations (12) and (13) of Kiseleva et al. (1998). Approximately 1000 systems were evolved for a time of $10 \times T_{Kozai}$, and considered as mergers if during the evolution the stars approached each other within a distance $r \leq R_1 + R_2$, i.e., their separation became smaller than the sum of their radii.

The parameters describing the mass and orbital distributions from which the initial conditions of the 3-body runs were drawn are given in Table 5. We adopted a fixed orbital apoapse of 0.03 pc , which corresponds approximately to the inner radial extent of the stellar disk at the Galactic center. Given its small apoapse, the eccentricity of the external orbit was chosen such that the periapsis distance to the MBH was uniform within the radial range $r_{p,out} \leq 10 r_{bt}$, or such that $r_{p,out} = 5 r_{bt}$.

The results of the simulations are shown in Table 6. For the highly inclined systems considered, the likelihood of a merger is $\approx 50\%$. Accounting for all possible inclinations, and for $r_{p,out} \leq 10 r_{bt}$ the merger probability is ≈ 0.16. We note that our results are similar to those obtained by Antonini et al. (2010). Our initial conditions and integrator are essentially the same as theirs with the difference that the equations of motion of Antonini et al. (2010) did not include terms accounting for dynamical effects due to tides. The similarity between the results of the two papers suggests that tides (as well as PN terms) have essentially no effect on the binary dynamics as expected if the binary angular momentum evolves substantially on a timescale of the order the binary orbital period.

A few examples are given in figure 9. The binary eccentricity increases as it orbits the Galactic center. Given the large eccentricity of the external orbit most of the evolution occurs during the binary closest approach to the MBH where the gravitational interaction is the strongest. The binary angular momentum receives a "kick" at each periapse passage, with two consecutive jumps separated roughly by the external orbital period of the binary. The step size of the angular momentum kick increases roughly as $\Delta\ell \sim \sqrt{1-e_1}$. These systems experience a clean “head-on” collision and their dynamics can be model quite accurately as it was purely Newtonian.

5. DISCUSSION

TABLE 6. Results of N-body simulations

fraction of systems	$r_{p,out} = 5r_{bt}$	$r_{p,out} \leq 10r_{bt}$
"mergers"	0.61	0.54
disrupted	0	0.12
binaries	0.39	0.46
integration T_{max}	$10 \times T_{Kozai}$	$10 \times T_{Kozai}$

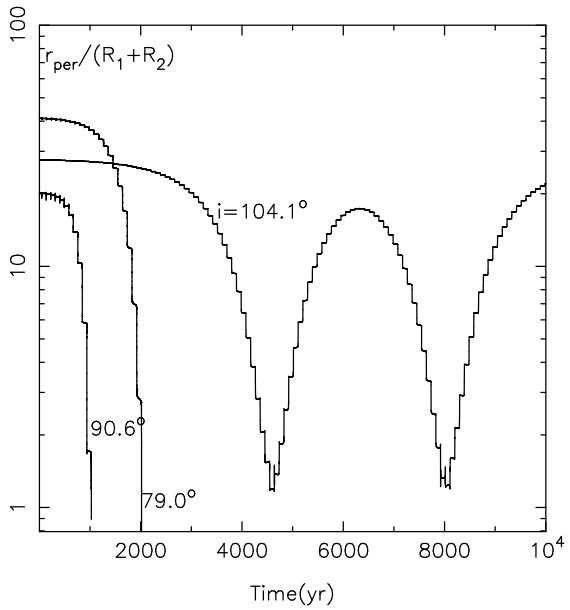

FIG. 9.— Example of N-body runs. The periapsis separation of the binary to the MBH was set to $r_{p,out} = 5r_{bt}$. When $r_{p,in}/(R_1+R_2) < 1$ systems are considered to have merged. $i_0 = 90^o.6$ corresponds to $m_1 = 1M_\odot$, $m_2 = 0.8M_\odot$, $a_1 = 0.38AU$; $i_0 = 79^o$ corresponds to $m_1 = 3M_\odot$, $m_2 = 3M_\odot$, $a_1 = 0.45AU$; $i_0 = 104^o.1$ corresponds to $m_1 = 1M_\odot$, $m_2 = 0.6M_\odot$, $a_1 = 0.26AU$.

Our results show that binary secular evolution could play a major role in their stelar evolution both on the MS as well as during their post-MS lifetime. In the following we briefly discuss several possible implications.

5.1. *Merger products*

5.1.1. *Blue stragglers and the observed mass function in the GC*

As shown in section 4, KCTF evolution and quasi-secular evolution can lead to binary mergers and collisions on the main-sequence. Such merger/collision products become "rejuvenated" stars, more massive than each of their original progenitors, and could possibly be observed as blue stragglers, as was originally suggested in (Perets & Fabrycky 2009; Perets 2009) and further investigated by Antonini et al. (2011) through hydrodynamical simulations.. However, given the complex stellar population of the GC showing evidence for continuous star formation, detecting such stars as blue-stragglers could be challenging. We note that such evolution will also lead to the formation of young massive merger products and might affect the observed mass-function of the OB stellar populations and further bias it to be top-heavy, and possibly explain the origin of the most massive S-stars.

5.1.2. *Post main-sequence evolution*

As discussed in Section 4.2 and shown in Table 4, KCTF evolution significantly affects the post-MS evolution of most (a significant fraction) of the KCTF-evolved binaries in the cusp (disk) models, leading to strong interactions between the binary components, mostly through mass-transfer and/or common envelope evolution. The exact actual outcome of such evolution depends on the secular dynamics that can still affect the binaries during their post-MS stage, which is not modelled here. However, these results already clearly show that the fraction of strongly-interacting binaries is likely to be significantly enhanced among stars in the GC close to the MBH. Such strongly interacting binaries could manifest themselves through a wide variety of outcomes, from progenitors of type Ia SNe, mass-transfer rejuvenated stars (i.e. in addition to the merger-produced rejuvenated stars in Section 5.1), as well as gravitational-wave sources (discussed in Antonini & Perets (2012)) and X-ray sources in accreting binaries, and may help explain the observed overabundance of the latter (Muno et al. 2005).

5.2. *G2-like objects as stellar merger products*

Gillessen et al. (2012, 2013) reported the discovery of G2, an extremely red object initially interpreted by these authors as a 3 Earth-mass gas cloud on a highly eccentric orbit with a closest approach to our Galaxy's central black hole expected to occur in mid March 2014. The orbit of G2 has an eccentricity of 0.98 and SMA of 0.03 pc. If the gas cloud interpretation is correct, G2 should be turned apart by the tidal field of the MBH as it passes through periapsis at a distance of 130 AU, potentially allowing us to observe with an unprecedented level of details an accretion event onto a MBH.

A number of authors have challenged the interpretation of G2 as a gas cloud and proposed instead alternative scenarios which invoke an underlying star (Miralda-Escudé 2012; Murray-Clay & Loeb 2012; Scoville & Burkert 2013). A stellar nature of G2 also appears to be in agreement with recent observations obtained on 2014 March 19 & 20 (UT). These observations show that G2, currently experiencing its closest approach, is still intact, in contrast to predictions for a simple gas cloud hypothesis (Ghez et al. 2014). Phifer et al. (2013) proposed that although G2 does have a gaseous component that is tidally interacting with the central black hole, there is likely a central star providing the self-gravity necessary to sustain the compact nature of the object. These authors argued that the G2's observed physical properties (red, compact, and at times marginally resolved) are consistent with the expected observables for stars which have recently undergone a merger. Following Phifer et al. (2013) we investigate here the possibility that G2 is the result of the merger of two stars. In our scenario, the G2 progenitors were initially part of a binary that was orbited by a distant third object, i.e., the initial system was a triple at an initial large distance from the GC. The triple was then scattered onto a quasi-radial orbit towards the GC through gravitational interactions with other stars or massive perturbers (Perets 2009). At the closest approach with the MBH the triple was dissociated leaving a binary onto an extremely eccentric and inclined orbit around the MBH. Such a binary merged due to the KL oscillations induced by its gravitational interaction with the MBH, producing an object with the peculiar features of G2.

A triple system that enters its tidal disruption radius leaves in $\sim 50\%$ of all cases a binary star around the MBH – in the other 50% of the cases the binary is ejected and its companion is captured (Bromley et al. 2006). The initial SMA of the

triple, a_{tr}, is obtained by requiring that the binary is left onto an orbit with external orbital periapsis roughly equal the tidal disruption radius of the triple, $r_{d,tr} = r_{p,out} \approx 130$ AU; this gives

$$a_{tr} \sim 1 \left(\frac{M_{tr}}{M_\bullet} \frac{4\times10^6 M_\odot}{3M_\odot} \right)^{1/3} \text{AU} . \quad (10)$$

with M_{tr} the total mass of the triple system. By requiring the triple to be initially stable (Mardling & Aarseth 2001), we obtain an upper limit to the semi-major axis of the binary a_1:

$$a_1 \lesssim \frac{a_{tr}\,(1-e_{tr})}{3.3} \left[\frac{2}{3} \left(1+\frac{m_3}{M_b} \right) \frac{1+e_{tr}}{(1-e_{tr})^{1/2}} \right]^{-2/5} \quad (11)$$
$$= 0.3 \frac{a_{tr}\,(1-e_{tr})}{\text{AU}} \left[\frac{2}{3} \left(1+\frac{m_3}{M_b} \right) \frac{1+e_{tr}}{(1-e_{tr})^{1/2}} \right]^{-2/5} \text{AU} ,$$

with e_{tr} the eccentricity of the outer companion with respect to the inner binary center of mass, M_b total mass of the inner binary and m_3 the mass of the third (ejected) star. The triple star parameters – an outer orbital distance of a few AU and a fraction of AU inner binary separation – required to give the observed orbit of G2 are therefore quite reasonable. For example if we assume a constant probability per $\ln(a_1)$ for $0.02 < a_1 < 20$ AU then the probability of finding a binary in the range of $0.02-0.1$AU is 10%; Fekel (1981) finds that a fraction of 0.2 of the more massive systems in close multiple stars have outer binary periods shorter than half a year, corresponding to $a_{tr} < 1$AU.

The binary will be left onto an orbit with a periapsis distance from the MBH that is a few times its tidal disruption radius. The SMA of the captured binary is:

$$a_{G2} \simeq 0.017 q \left(\frac{M_\bullet}{4\times10^6 M_\odot} \right) \left(\frac{1000\text{km s}^{-1}}{v_{ej}} \right)^2 \text{pc} , \quad (12)$$

where $q = M_{G2}/m_3$, with M_{G2} being a mass of G2 and corresponding to M_b, and v_{ej} is the velocity at infinity of the ejected star. In agreement with a triple disruption origin for G2, its orbit SMA is comparable to the orbital radii inside of the S-stars that are thought to be deposited at the GC through binary disruptions by the MBH (Hills 1988). The characteristic eccentricity of the binary orbit depends on q and the mass ratio of the binary to the MBH (Zhang et al. 2013):

$$e_{G2} \sim 1 - \frac{2.8}{q^{1/3}(1+q)^{2/3}} \left(\frac{M_{G2}}{M_\bullet} \right)^{1/3} , \quad (13)$$

which gives $e_{G2} = 0.98$ for $q = 1$ and $M_{G2}/M_\bullet = 5\times10^{-7}$. It is notable that the triple disruption scenario followed by a merger of the captured binary, naturally reproduces G2 observationally derived SMA, ~ 0.03 pc, and eccentricity, 0.98. The orbital evolution of the binary following its capture around the MBH will resemble that of the systems of Fig. 9 – the two stars will merge on a timescale of order $\sim 10^3-10^4$ yr, provided that the mutual inclination between outer and inner orbit is large.

We add that the observed properties of G2 are not far different from those of several observed stellar objects that are thought to have formed through a stellar merger. For example, G2 temperature and radius are similar to those of BLG-360 recently observed by Tylenda et al. (2013). Also V4332 Sgr (Kamiński et al. 2010) as well as V1309 Sco (Zhu et al. 2013) at present are strong IR sources with a similar dust temperature as G2. Also the well known red-nova V838 Mon (Kamiński et al. 2009) although looks different from G2, as an M6 component dominates, it is also bright in IR and it is quite probable that if oriented in a different way than observed, i.e. that denser dust region obscures the central object, it would also be observed as similar to G2. CK Vul (Nova Vul 1670) it is also likely to have been a stellar merger and now is seen only as an infrared source (Kato 2003). If correctly interpreted, CK Vul shows that the evolution of stellar merger remnants are slow, so the G2 merger could have happened hundreds or thousands of years ago. In fact, when two similar stars merge the remnant resembles a pre-MS star and evolves on a similar time scale.

The main question is whether these mergers are common enough such that there is a finite probability of observing one object with the characteristics of G2 at any time in the GC. We evaluate the event rate for mergers produced by triple disruptions followed by KL evolution of the captured binary as:

$$\Gamma_m = \Gamma_b \times f_{tr} \times f_b \times f_m , \quad (14)$$

where Γ_b is the tidal disruption event rate for binaries at the GC, f_{tr} is the fraction of binaries in triple systems, f_b is the fraction of events that leave a binary around the MBH and f_m is the fraction of these systems that end up merging. We take $\Gamma_b = 10^{-4}\text{yr}^{-1}$ as this is roughly the production rate required to obtain the observed number of S-stars (~ 20) within a radius of 0.05 pc of SgrA* (Perets et al. 2007). From the simulations of Section 4.3 we have $f_m \approx 0.1$. We set $f_b = 0.5$ and following Perets (2009) we assume a triple fraction of $f_{tr} = 0.2$. With these values we find $\Gamma_m \approx 10^{-6}\text{yr}^{-1}$. The merger product can look like G2 only before it contracts back to the MS and continues its evolution as a normal MS star. The thermal timescale over which the star will reach the main-sequence is of order $\sim 10^5$yr (see Table 6 of Antonini et al. 2011), so the probability of finding a merger product out of thermal equilibrium at any time in the GC is roughly ~ 0.1. We note however that the continuous tidal interaction of the puffed-up merger product with the MBH could keep the star from reaching thermal equilibrium. In such a scenario the merger product could maintain properties similar to G2 for a time much longer than 10^5yr, increasing its chance of being observed with such properties.

6. SUMMARY

In this study we explored the secular evolution of main sequence binaries around a massive black hole taking into account tidal effects of the inner binary and the interaction of the binaries with the stellar environment. The later stellar evolution of the dynamically evolved binaries was also explored, albeit simplistically. We considered binaries in the observed young stellar disk, as well as binaries in the old stellar cusp. For both cases we took into account two possible density profiles; a cusp, and a core-like profile. We find that the MBH can induce very high eccentricities in the orbits of binaries around it, causing them to coalesce or significantly evolve through tidal evolution and/or later stellar evolution (common envelope, mass transfer etc.), on timescales shorter than the evaporation time of the binaries around the MBH. The main results of our study are summarized below:

- The dynamics of binaries with high inclinations with respect to their orbit around the MBH ($70^\circ \lesssim i \lesssim 110^\circ$) are strongly affected by KCTF leading to the shrinking of the binary SMA, at distances up to 0.5 pc from the MBH. As a consequence of a shorter SMA, the binaries' evaporation time becomes longer and their survival rate is enhanced by $\sim 10\%$ in the GC environment.

- 2-3 % of all binaries are likely to merge due to secular evolution on the main sequence. Mergers during the main-sequence evolution of the binaries typically occur through high excitation of eccentricity leading to direct physical collision before tidal dissipation can become important to the evolution.

- The post-MS evolution of the majority of the binaries that suffered secular evolution during the MS phase is significantly altered by KCTF which can lead to strong binary interaction through mass-exchange and/or common-envelope evolution. As a result, this could enhance the fraction of X-ray sources in the GC, and may offer an explanation for the overabundance of X-ray sources in the GC.

- Merger products and mass-transfer systems could produce rejuvenated stars ("blue stragglers") and affect the observed mass function of the GC stars in both the young disk and the stellar cusp.

- We suggest that the recently observed G2-cloud in the GC could potentially be the product of a binary merger due to KL cycles induced by the central MBH.

Authors are grateful to Cole Miller, Romuald Tylenda and Noam Soker for helpful discussions.This research has made use of the SIMBAD database, operated at CDS, Strasbourg, France, and of NASA's Astrophysics Data System. SP is supported in part by NSERC of Canada. HBP acknowledges support from the Technion Deloro fellowship and the I-CORE Program of the Planning and Budgeting Committee and The Israel Science Foundation grant 1829/12.

REFERENCES

Alexander, T. 2005, Phys. Rep., 419, 65
Antognini, J. M., Shappee, B. J., Thompson, T. A., & Amaro-Seoane, P. 2014, MNRAS, 439, 1079
Antonini, F., Faber, J., Gualandris, A., & Merritt, D. 2010, ApJ, 713, 90
Antonini, F., Lombardi, Jr., J. C., & Merritt, D. 2011, ApJ, 731, 128
Antonini, F., Murray, N., & Mikkola, S. 2014, ApJ, 781, 45
Antonini, F., & Perets, H. B. 2012, ApJ, 757, 27
Bartko, H., et al. 2009, ApJ, 697, 1741
—. 2010, ApJ, 708, 834
Binney, J., & Tremaine, S. 2008, Galactic Dynamics: Second Edition (Princeton University Press)
Blaes, O., Lee, M. H., & Socrates, A. 2002, ApJ, 578, 775
Bromley, B. C., Kenyon, S. J., Geller, M. J., Barcikowski, E., Brown, W. R., & Kurtz, M. J. 2006, ApJ, 653, 1194
Buchholz, R. M., Schödel, R., & Eckart, A. 2009, A&A, 499, 483
Do, T., Ghez, A. M., Morris, M. R., Lu, J. R., Matthews, K., Yelda, S., & Larkin, J. 2009, ApJ, 703, 1323
Duquennoy, A., & Mayor, M. 1991, A&A, 248, 485
Eggleton, P. 2006, Evolutionary Processes in Binary and Multiple Stars
Eggleton, P. P., & Kiseleva-Eggleton, L. 2001, ApJ, 562, 1012
Fabrycky, D., & Tremaine, S. 2007, ApJ, 669, 1298
Fekel, Jr., F. C. 1981, ApJ, 246, 879
Ford, E. B., Kozinsky, B., & Rasio, F. A. 2000, ApJ, 535, 385
Ghez, A. M., et al. 2008, ApJ, 689, 1044
Gillessen, S., Eisenhauer, F., Trippe, S., Alexander, T., Genzel, R., Martins, F., & Ott, T. 2009, ApJ, 692, 1075
Gillessen, S., et al. 2012, Nature, 481, 51
—. 2013, ApJ, 763, 78
Hamers, A. S., Pols, O. R., Claeys, J. S. W., & Nelemans, G. 2013, MNRAS, 430, 2262
Hills, J. G. 1988, Nature, 331, 687
Holman, M., Touma, J., & Tremaine, S. 1997, Nature, 386, 254
Hopman, C., & Alexander, T. 2006, ApJ, 645, L133
Hurley, J. R., Pols, O. R., & Tout, C. A. 2000, MNRAS, 315, 543
Kamiński, T., Schmidt, M., & Tylenda, R. 2010, A&A, 522, A75
Kamiński, T., Schmidt, M., Tylenda, R., Konacki, M., & Gromadzki, M. 2009, ApJS, 182, 33
Kato, T. 2003, A&A, 399, 695
Katz, B., & Dong, S. 2012, arXiv:astro-ph/1211.4584
Kiseleva, L. G., Eggleton, P. P., & Mikkola, S. 1998, MNRAS, 300, 292
Kozai, Y. 1962, AJ, 67, 591
Lidov, M. L. 1962, Planet. Space Sci., 9, 719
Lu, J. R., Do, T., Ghez, A. M., Morris, M. R., Yelda, S., & Matthews, K. 2013, ApJ, 764, 155
Lu, J. R., Ghez, A. M., Hornstein, S. D., Morris, M. R., Becklin, E. E., & Matthews, K. 2009, ApJ, 690, 1463
Mardling, R. A., & Aarseth, S. J. 2001, MNRAS, 321, 398
Mazeh, T., & Shaham, J. 1979, A&A, 77, 145
Mikkola, S., & Merritt, D. 2008, AJ, 135, 2398
Miller, M. C., & Hamilton, D. P. 2002, ApJ, 576, 894
Miralda-Escudé, J. 2012, ApJ, 756, 86
Muno, M. P., Pfahl, E., Baganoff, F. K., Brandt, W. N., Ghez, A., Lu, J., & Morris, M. R. 2005, ApJ, 622, L113
Murray-Clay, R. A., & Loeb, A. 2012, Nature Communications, 3
Naoz, S., & Fabrycky, D. 2014, arXiv:astro-ph/1405.5223
Naoz, S., Farr, W. M., Lithwick, Y., Rasio, F. A., & Teyssandier, J. 2013a, MNRAS, 431, 2155
Naoz, S., Kocsis, B., Loeb, A., & Yunes, N. 2013b, ApJ, 773, 187
Perets, H. B. 2009, ApJ, 698, 1330
Perets, H. B., & Fabrycky, D. C. 2009, ApJ, 697, 1048
Perets, H. B., & Gualandris, A. 2010, ApJ, 719, 220
Perets, H. B., Hopman, C., & Alexander, T. 2007, ApJ, 656, 709
Perets, H. B., & Kratter, K. M. 2012, ApJ, 760, 99
Perets, H. B., & Naoz, S. 2009, ApJ, 699, L17
Phifer, K., et al. 2013, ApJ, 773, L13
Prodan, S., & Murray. 2014, arXiv:astro-ph/1411.0368
Prodan, S., & Murray, N. 2012, ApJ, 747, 4
Prodan, S., Murray, N., & Thompson, T. A. 2013, arXiv:astro-ph/1305.2191
Salpeter, E. E. 1955, ApJ, 121, 161
Schödel, R., Merritt, D., & Eckart, A. 2009, A&A, 502, 91
Scoville, N., & Burkert, A. 2013, ApJ, 768, 108
Tylenda, R., et al. 2013, A&A, 555, A16
Wu, Y., & Murray, N. 2003, ApJ, 589, 605
Zhang, F., Lu, Y., & Yu, Q. 2013, ApJ, 768, 153
Zhu, C., Lü, G., & Wang, Z. 2013, ApJ, 777, 23